

Evaluating Planetary Boundary Layer Parameterizations in HWRF using Aircraft Observations

A Project Report to 2019 DTC Visitor Program

Jun A. Zhang

University of Miami & NOAA/AOML/Hurricane Research Division

(Email: jun.zhang@noaa.gov)

1. Background

Tropical cyclone (TC) intensity is controlled by both environmental and internal processes. These processes are required to be correctly represented in TC forecast models in order to advance intensity forecasts. Due to continuous reduction in the resolution of operational TC forecast models, physical parameterizations traditionally used in the low-resolution models may not be suitable. Turbulent mixing is known to play an essential role in TC simulations according to theoretical studies (e.g., Bryan 2012; Zhang and Marks 2015; Zhang et al. 2018). Previous numerical studies also showed that the simulated TC intensity and structure are largely influenced by the planetary boundary layer (PBL) schemes that parameterize turbulent processes (e.g., Emanuel 1995; Braun and Tao 2000; Foster 2009; Nolan et al. 2009; Smith and Thomsen 2010; Kepert 2012). Zhang et al. (2015) demonstrated that the forecasted TC intensity and structure are sensitive to the vertical eddy diffusivity (K_m) in the planetary boundary layer (PBL) scheme of the operational Hurricane Weather and Research Forecast (HWRF) model.

In the current version of the operational HWRF model, the Eddy-diffusivity and Mass-flux (EDMF) PBL scheme is used, in which the vertical eddy diffusivity for momentum flux is formulated as:

$$K_m = k (u^*/\Phi_m) Z \alpha (1 - Z/h)^2, \quad (1)$$

where k is the Von Kármán constant ($k=0.4$), u^* is the surface frictional velocity scale, Φ_m is the stability function evaluated at the top of the surface layer, Z is the height above the surface, and h is the PBL height that is determined using the critical Richardson number (Ri_{cr}) method. Note that there is no mass-flux component in the PBL scheme of HWRF before 2016.

The tuning parameter, α , was set to 1 in 2011 version and earlier versions of HWRF (H11). It was set to 0.5 in the 2012 version (H12, Zhang et al. 2012; Gopalakrishnan et al. 2013), and 0.75 in the 2013 and 2014 versions (H13-14). In the 2015 version (H15), α varied with the wind speed (Bu et al. 2017), while in the 2016-2018 versions (H16-18), it was set as a function of both wind speed and height (Wang et al. 2018).

Until now, the way in which the PBL schemes in different versions of HWRF affect TC's intensity and structure has not been well documented. Besides the HWRF PBL schemes, impacts of other schemes on HWRF simulations of TCs, such as the Yonsei University (YSU) PBL scheme (Hong et al. 2006) and MYNN scheme which is a modified version of the Mellor and Yamada (1982) scheme by Nakanishi and Nino (2006) remain to be understood. Note that there is no α parameter in the YSU and MYNN schemes.

2. Objectives

The long-term goal is to improve HWRF's performance for TC intensity forecasts. The goal of this project is to evaluate PBL parameterization schemes in HWRF simulations based on the best available observations. Specifically, the objectives are:

- 1) To evaluate the impacts of different HWRF PBL schemes on TC intensity and structure.
- 2) To evaluate the impacts of the YSU and MYNN schemes on the boundary-layer structure, in comparison to the latest HWRF scheme and observations.

3. Results summary

Our model diagnostics followed a developmental framework for improving model physics (Zhang et al. 2012). This framework includes four steps: model diagnostics, physics development, physics upgrade and further evaluation. Model deficiencies were identified through model diagnostics by comparing the simulated TC structures to observations. We focused on comparisons of the TC structures in idealized HWRF simulations with different PBL schemes. Note that only the PBL scheme is different, while the boundary and initial conditions as well other physics are the same in these simulations. We developed structural metrics based on aircraft observations for model evaluation purposes. These structural metrics include storm size, maximum inflow strength, boundary layer heights, warm-core anomaly and height, and distribution of convective bursts. The simulated TC structures were compared to available observation composites.

Figure 1 shows the simulated TC intensity in terms of the maximum surface wind speed (V_{max}) from 8 numerical experiments, including simulations with 5 versions of HWRF PBL schemes (i.e., H11, H12, H13-14, H15, and H16-18), EDMF, YSU and MYNN schemes. It is evident from Fig. 1 that both the extent of intensification during the rapid intensification (RI) period (12-36 h) and the maximum intensity of the 5-day simulations are different among these experiments. The storm in H15 is the strongest, while that in the simulation with the original EDMF scheme is the weakest. Among HWRF PBL schemes, H11 produces the weakest storm.

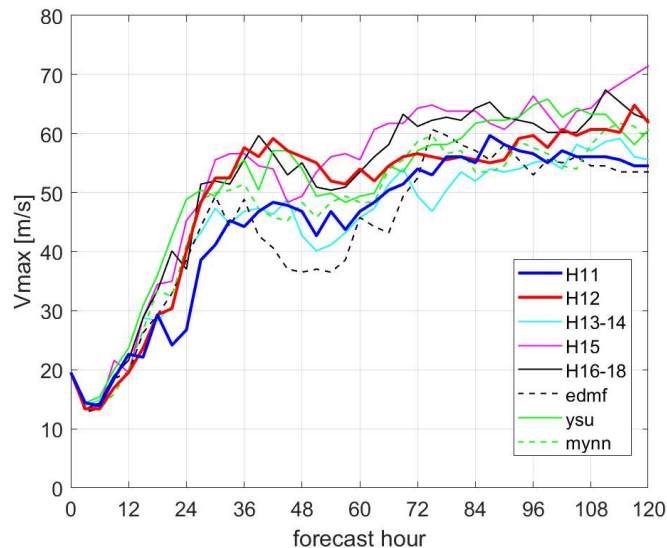


Figure 1: Time series of simulated storm intensity in idealized HWRF simulations with different PBL schemes.

During the RI period, the magnitude of the azimuthal averaged inflow correlates well with the storm intensity (Figs. 1 and 2). The strength of the peak inflow in H15 is nearly twice that in H11. Note that K_m is the largest in H15, while it is the smallest in H11. This result confirms that K_m regulates the TC inflow strength. The difference in the inflow strength in these simulations are tied to the storm size difference. Figure 3 shows radial profiles of the azimuthally averaged wind speed at 10 m altitude during the RI period in these 5 simulations. Not only the maximum V_t but also the radius of the maximum wind speed (RMW) are different in these simulations. The larger the inflow strength, the smaller the storm size. The storm size is also linked to the magnitude of K_m in that the RMW is smaller in the simulation with smaller K_m .

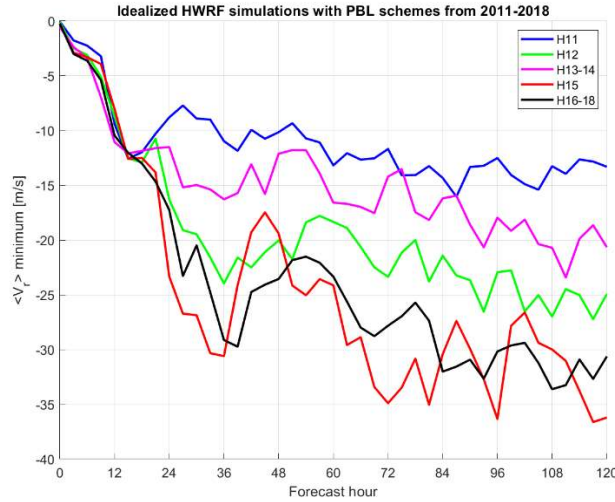


Figure 2: Minimum azimuthally averaged radial wind speed (V_r) in the idealized simulations with different versions of HWRF PBL schemes.

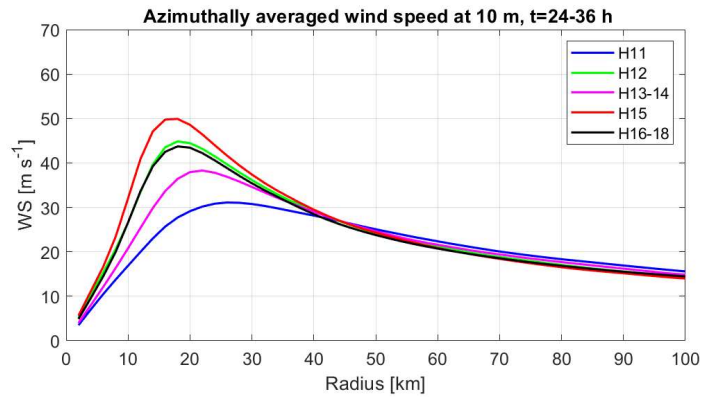


Figure 3: Radial profiles of azimuthally averaged 10 m wind speed in the idealized simulations with different versions of HWRF PBL schemes.

We then compare the boundary-layer heights in the simulations with observational composites from Zhang et al. (2011). Figure 4 shows the azimuthally averaged tangential wind speed (V_t) normalized by the maximum value in simulations with HWRF PBL schemes and observation composite. The black line in each panel of Fig. 4 represents the height of the maximum V_t . The increase of this height scale with radius is seen in all simulations. This height

scale is the largest in H11 right outside the eyewall while it is the smallest in H15. The boundary layer height is similar in H15 and H16-18, which matches the observations better than that in other simulations.

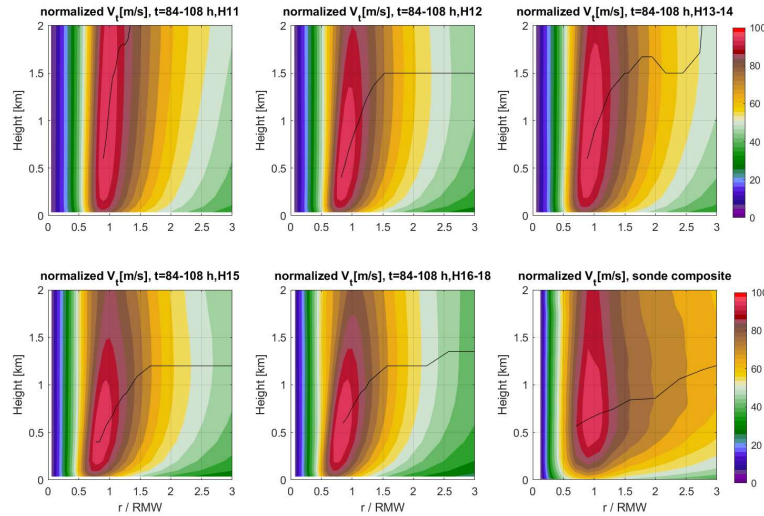


Figure 4: Radius-height plot of the normalized tangential wind speed by the maximum value (in %) in idealized HWRf simulations and observation composite.

Similarly, Figure 5 shows the normalized radial wind speed (V_r) by the minimum V_r . The inflow layer depth is defined as the height of 10% peak inflow and is denoted by the black line in each panel of Fig. 5. The increase of the inflow layer depth with radius is shown in all simulations in agreement with observations. H15 and H16-18 simulated the inflow layer depth better than other experiments in comparison to the dropsonde composite.

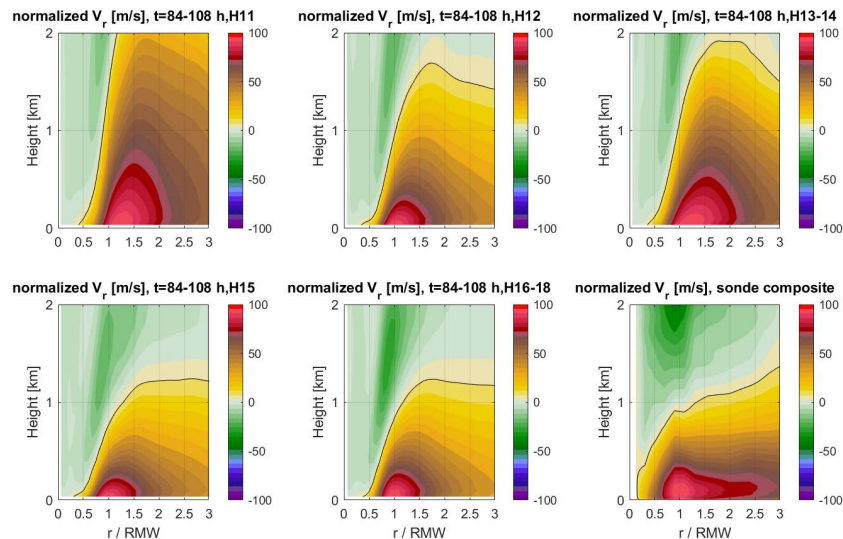


Figure 5: Radius-height plot of the normalized radial wind speed by the minimum value (in %) in idealized HWRf simulations and observation composite.

These results in Figs. 4 and 5 suggest that recent PBL upgrades in HWRF improve the representation of the kinematic boundary layer height. Of note, the inflow layer depth is similar in YSU and MYNN simulations compared to that in the H16-18 simulation (Fig. 6).

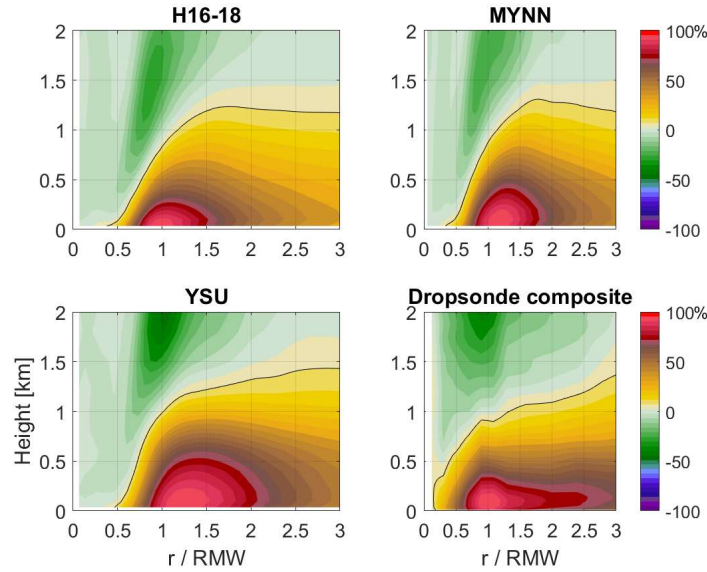


Figure 6: Radius-height plot of the normalized radial wind speed by the minimum value in H16-18, YSU and MYNN simulations, and observation composite.

Figure 7 compares the thermodynamic boundary layer height in these simulations and observation composite. This height scale is defined as where vertical gradient of virtual potential temperature (θ_v) is 3 K/km. The thermodynamic PBL height is similar among the five experiments, which is all deeper than in the observation composite. This result indicates that the thermodynamic structure remains to be improved in HWRF.

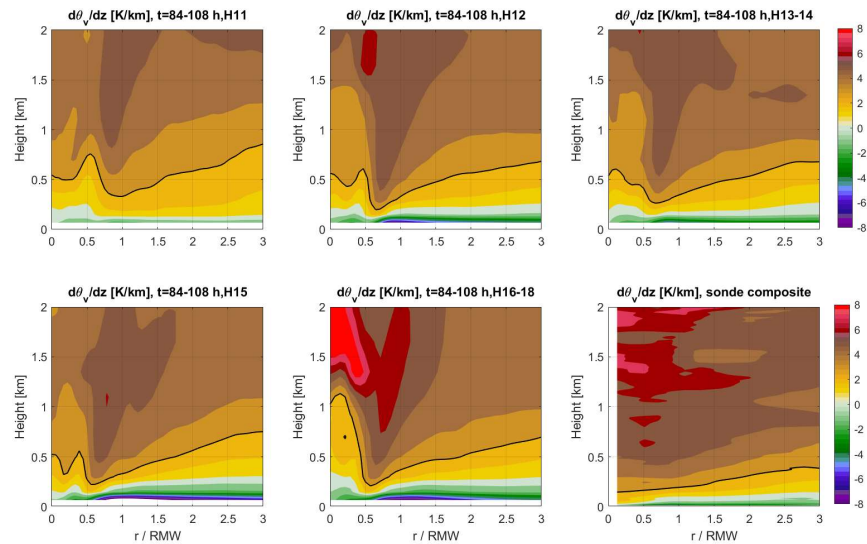


Figure 7: Radius-height plot of the vertical lapse rate in idealized HWRF simulations and observation composite.

The evolution of the warm-core anomaly in the five simulations with HWRP PBL schemes is compared in Fig. 8. Both the magnitude and height of the maximum anomaly are different in these simulations. The warm-core anomaly is larger in H15 and H16-18 when the storm intensity is stronger than in other simulations. There is no relationship between the warm-core height and storm intensity. Double warm core structure is seen in all simulations except H16-18. It is possible that the mass flux component of the H16-18 scheme caused this difference in the warm-core structure.

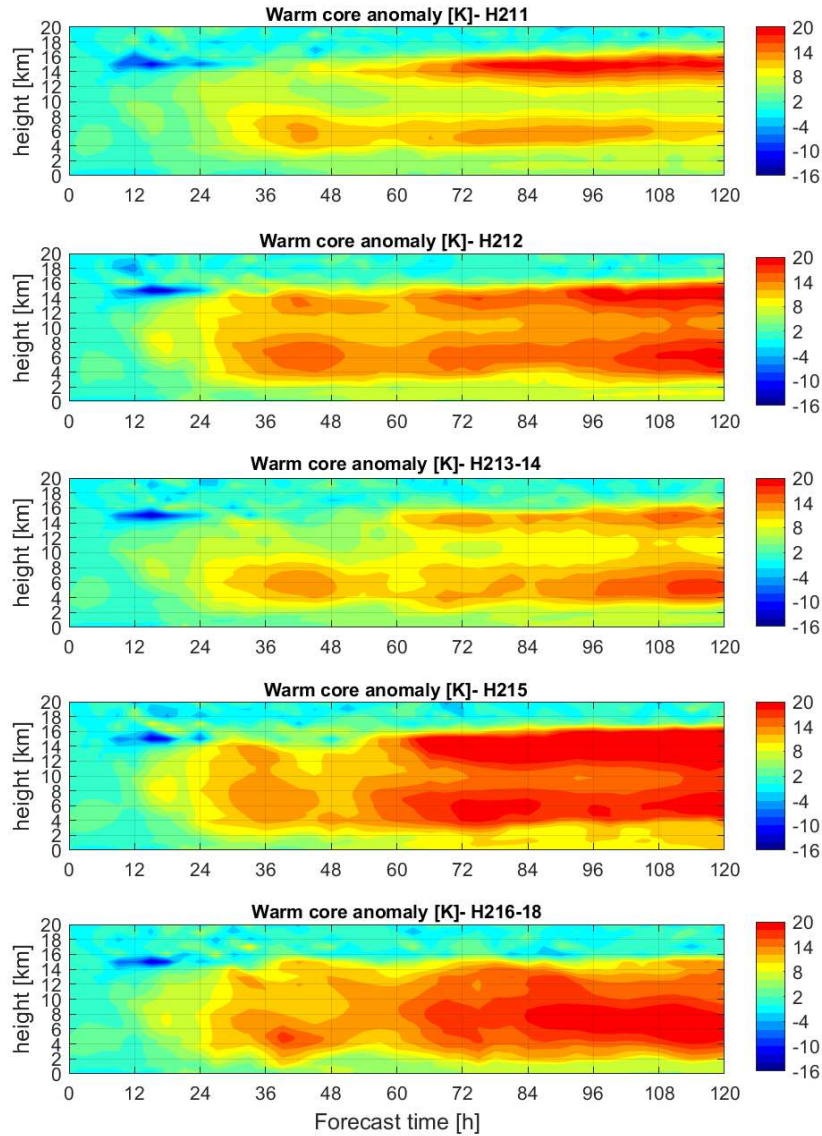


Figure 8: Evolution of the warm-core anomaly in simulations with HWRP PBL schemes.

Counts of convective bursts in the RI period are compared in these HWRP simulations in Fig. 9. The total number of bursts is the largest in H15, while it is the smallest in H11. More bursts are located inward from the RMW in stronger storm simulations with smaller K_m . This result agrees with previous numerical and observational findings (e.g., Nolan et al. 2007; Rogers et al. 2013; Zhang and Rogers 2019).

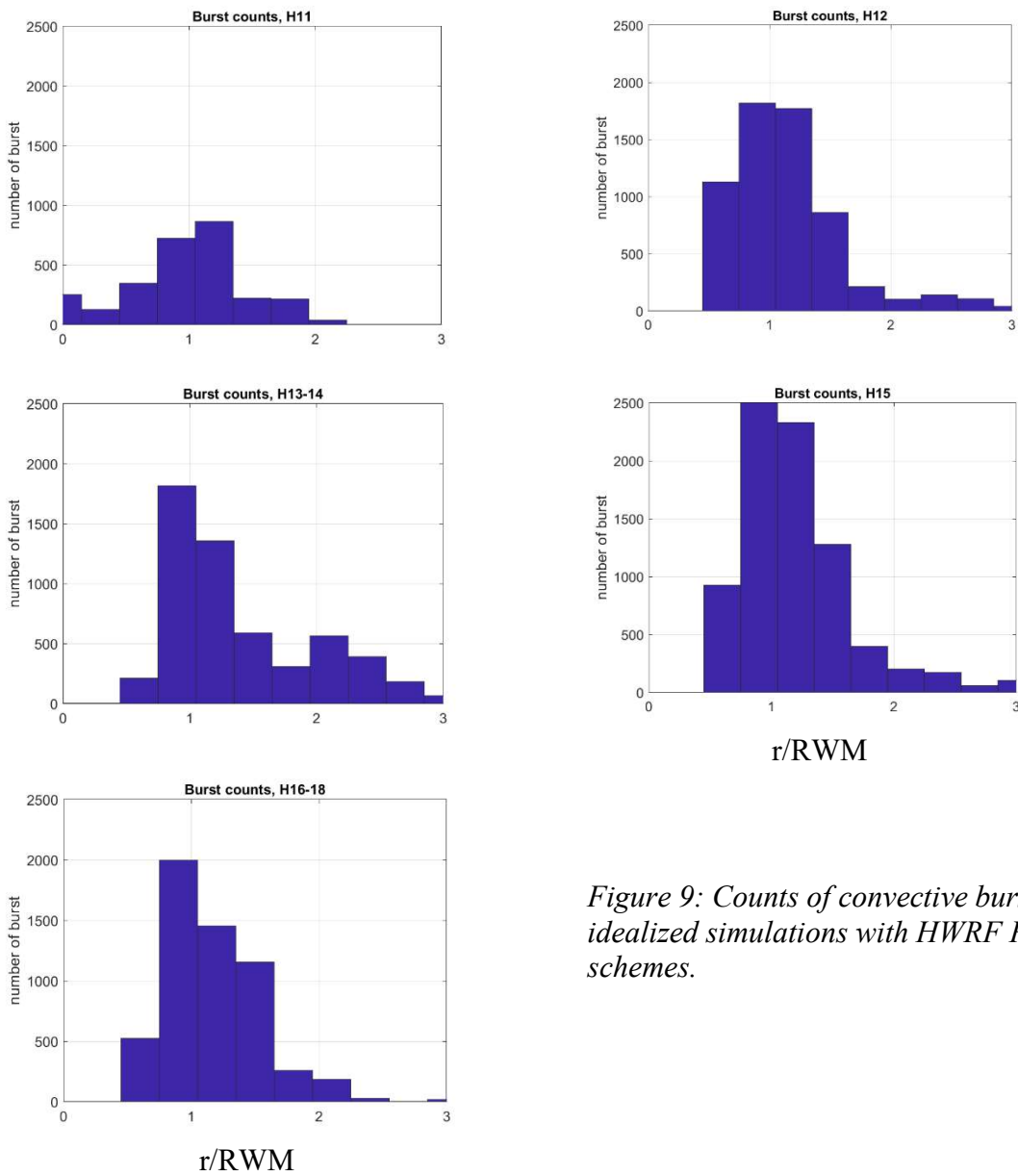


Figure 9: Counts of convective bursts in the idealized simulations with HWRP PBL schemes.

The simulated low-level temperature and humidity are compared in Figs. 10 and 11, respectively, showing similar structures. Near the surface, the simulated temperature and humidity are comparable to observations. However, the upper boundary layer is found to be too cool and dry in all simulations with HWRP PBL schemes compared to observations. A similar result is found in YSU and MYNN simulations (Fig. 12). Although the simulated structure is closest to observations in H16-18, the dry and cool bias are still observed. This result suggests that future PBL physics upgrade in HWRP should focus on improvement of the thermal structure in TC forecasts. Note that detailed comparisons of the TC structure and observations are summarized in Zhang et al. (2020).

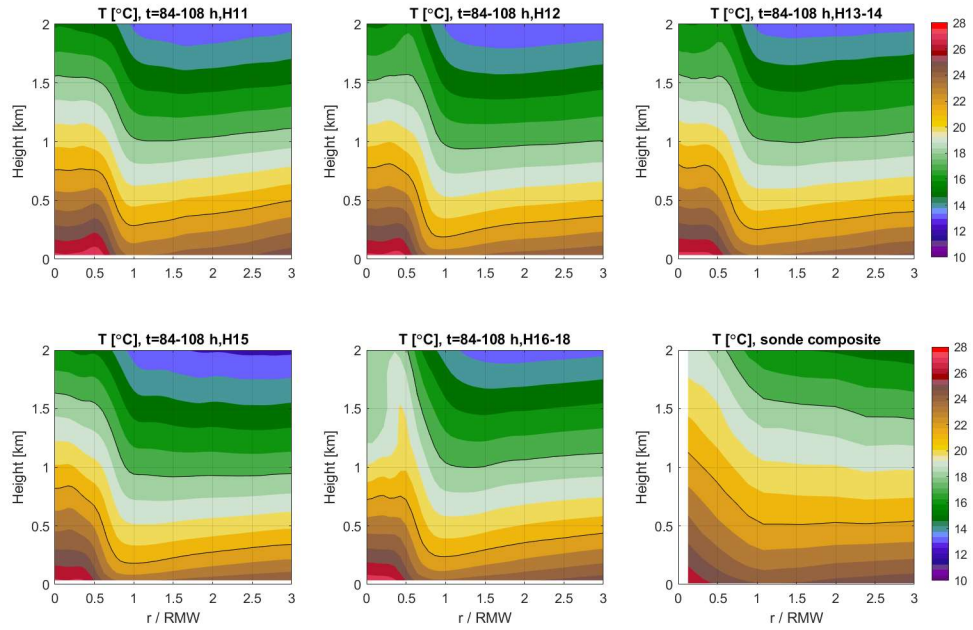


Figure 10: Radius-height plot of temperature from simulations with HWRP PBL schemes and dropsonde composite.

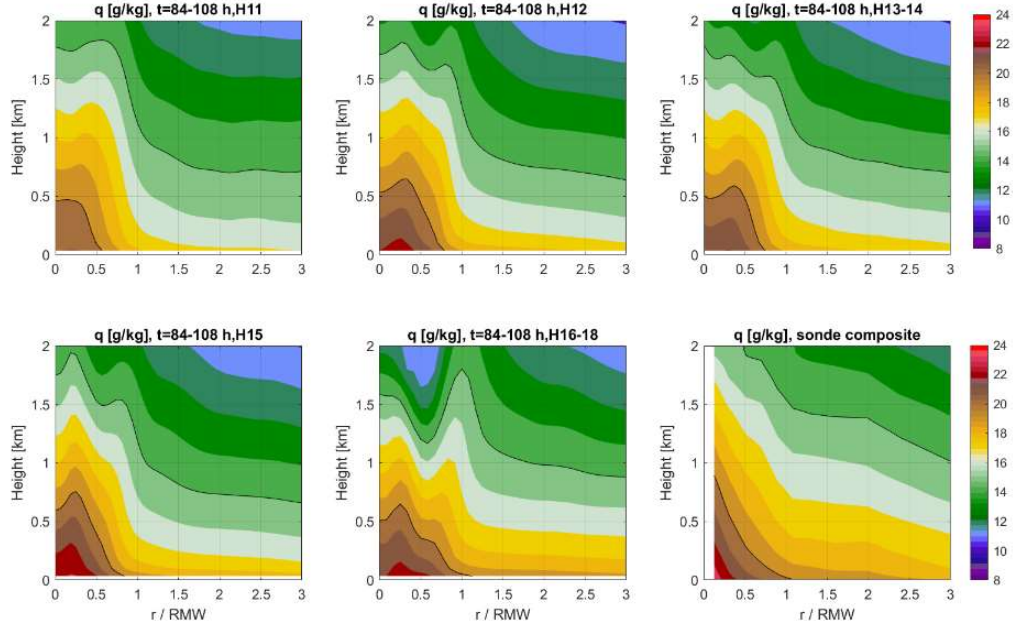


Figure 11: Radius-height plot of humidity from simulations with HWRP PBL schemes and dropsonde composite.

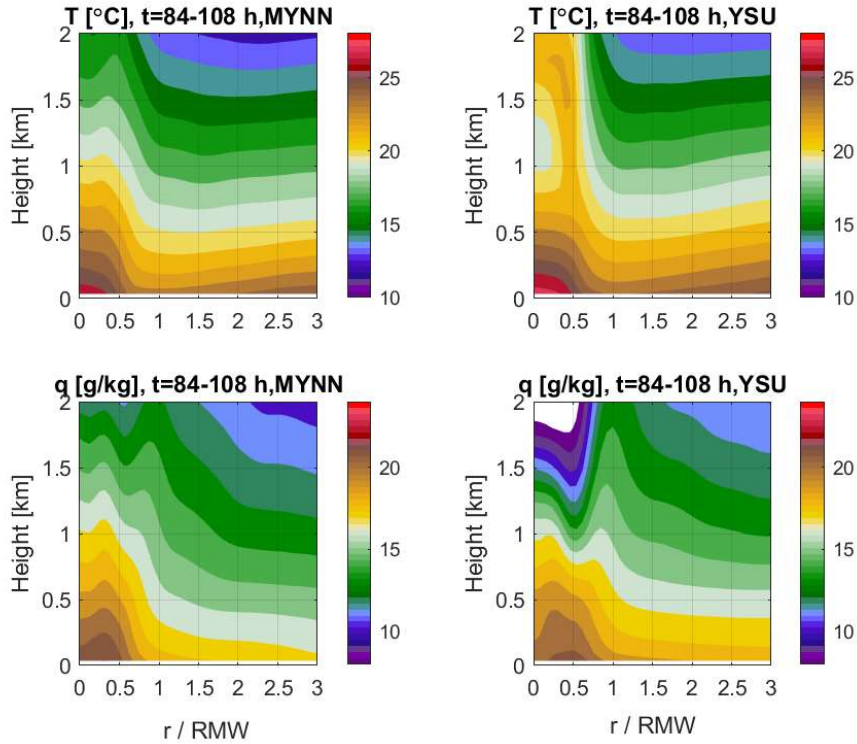


Figure 12: Radius-height plot of temperature and humidity from simulations with MYNN and YSU schemes.

4. Conclusions

In this project, we evaluated the impacts of different PBL schemes on HWRP forecasts of TC's intensities. We found that the 2011 version PBL scheme in HWRP produced the weakest storm, while the 2015 version produced the strongest storm. The YSU and MYNN schemes produced TCs with a similar intensity as the 2016-18 HWRP PBL scheme. The simulated storm intensity is anti-correlated with the magnitude of the vertical eddy diffusivity.

The simulated TC structure is also sensitive to the PBL scheme. The inflow is much stronger in H16-18 and H15 simulations than in H13-14 and H11 simulations. The boundary layer is shallower in the H16-18 simulation than in earlier versions of the HWRP PBL schemes. The simulated boundary layer structure in MYNN and YSU simulations are comparable to that in the H16-18 simulation. Compared to observations, the results suggested that upgrades in the latest two versions of HWRP improved the simulated kinematic structure. However, dry and cool biases in the upper boundary layer were identified in all simulations compared to observations. Thus, we recommend model developers pay attention to the thermodynamic structure in future upgrades of the HWRP physics.

5. References:

- Braun, S. A., and W.-K. Tao, 2000: Sensitivity of high-resolution simulations of Hurricane Bob (1991) to planetary boundary layer parameterizations. *Mon. Wea. Rev.*, **128**, 3941–3961.
- Bryan, G. H., 2012: Effects of surface exchange coefficients and turbulence length scales on the intensity and structure of numerically-simulated hurricanes. *Mon. Wea. Rev.*, **140**, 1125–1143.
- Bu, Y. P., R. G. Fovell, and K. L. Corbosiero, 2017: The influences of boundary layer vertical mixing and cloud-radiative forcing on tropical cyclone size. *J. Atmos. Sci.*, **74**, 1273–1292.
- Emanuel, K. A., 1995: Sensitivity of tropical cyclones to surface exchange coefficients and a revised steady-state model incorporating eye dynamics. *J. Atmos. Sci.*, **52**, 3969–3976.
- Foster, R. C., 2009: Boundary-layer similarity under an axisymmetric, gradient wind vortex. *Boundary-Layer Meteorol.*, **131**, 321–344.
- Gopalakrishnan, S. G., F. D. Marks, Jr, J. A. Zhang, X. Zhang, J.-W. Bao and V. Tallapragada, 2013: A study of the impacts of vertical diffusion on the structure and intensity of tropical cyclones using the high resolution HWRF system. *J. Atmos. Sci.*, **70**, 524–541.
- Hong, S., Y. Noh, and J. Dudhia, 2006: A new vertical diffusion package with an explicit treatment of entrainment processes. *Mon. Wea. Rev.*, **134**, 2318–2341.
- Kepert, J. D., 2012: Choosing a boundary layer parameterization for tropical cyclone modeling. *Mon. Wea. Rev.*, **140**, 1427–1445.
- Mellor, G. L., and T. Yamada, 1982: Development of a turbulence closure model for geophysical fluid problems. *Rev. Geophys.*, **20**, 851–875.
- Nakanishi, M., and H. Niino, 2006: An improved Mellor–Yamada level-3 model: Its numerical stability and application to a regional prediction of advection fog. *Boundary-Layer Meteorol.*, **119**, 397–407.
- Nolan, D. S., Y. Moon, and D. P. Stern, 2007: Tropical cyclone intensification from asymmetric convection: Energetics and efficiency. *J. Atmos. Sci.*, **64**, 3377–3405.
- Nolan D. S., J. A. Zhang, and D. P. Stern, 2009: Evaluation of planetary boundary layer parameterizations in tropical cyclones by comparison of in-situ data and high-resolution simulations of Hurricane Isabel (2003). Part I: Initialization, maximum winds, and outer core boundary layer structure. *Mon. Wea. Rev.*, **137**, 3651–3674.
- Rogers, R. F., P. Reasor, and S. Lorsolo, 2013: Airborne Doppler observations of the inner-core structural differences between intensifying and steady-state tropical cyclones. *Mon. Wea. Rev.*, **141**, 2970–2991.
- Smith, R. K., and G. L. Thomsen, 2010: Dependence of tropical cyclone intensification on the boundary layer representation in a numerical model. *Quart. J. Roy. Meteor. Soc.*, **136**, 1671–1685.
- Wang, W., J. A. Sippel, S. Abarca, L. Zhu, B. Liu, Z. Zhang, A. Mehra and V. Tallapragada, 2018: Improving NCEP HWRF simulations of surface wind and inflow angle in the eyewall area. *Weather Forecasting*, **33**, 887–898.
- Zhang, J. A., and F. D. Marks, 2015: Effects of horizontal diffusion on tropical cyclone intensity change and structure in idealized three-dimensional numerical simulations. *Mon. Wea. Rev.*, **143**, 3981–3995.
- Zhang, J. A., F. D. Marks, J. A. Sippel, R. F. Rogers, X. Zhang, S. G. Gopalakrishnan, Z. Zhang, and V. Tallapragada, 2018: Evaluating the impact of improvement in the horizontal diffusion parameterization on hurricane prediction in the operational Hurricane Weather Research and Forecasting (HWRF) model. *Wea. Forecasting*, **33**, 317–329.

- Zhang, J. A., S. G. Gopalakrishnan, F. D. Marks, R. F. Rogers, and V. Tallapragada, 2012: A developmental framework for improving hurricane model physical parameterizations using aircraft observations. *Trop. Cycl. Res. Rev.*, 1 (4): 419-429.
- Zhang, J. A., E. A. Kalina, M. K. Biswas, R. F. Rogers, P. Zhu, F. D. Marks, 2020: A Review and Evaluation of Planetary Boundary Layer Parameterizations in Hurricane Weather Research and Forecast Model using Idealized Simulations and Observations. *Atmosphere*, in review.
- Zhang, J. A., D. S. Nolan, R. F. Rogers, and V. Tallapragada, 2015: Evaluating the impact of improvements in the boundary layer parameterizations on hurricane intensity and structure forecasts in HWRF. *Mon. Wea. Rev.*, **143**, 3136-3154.
- Zhang, J. A., R. F. Rogers, D. S. Nolan, and F. D. Marks, 2011: On the characteristic height scales of the hurricane boundary layer. *Mon. Wea. Rev.*, **139**, 2523-2535.
- Zhang, J. A., and R. F. Rogers, 2019: Effects of parameterized boundary layer structure on hurricane rapid intensification in shear. *Mon. Wea. Rev.*, **147**, 853-871.